

See discussions, stats, and author profiles for this publication at: <https://www.researchgate.net/publication/326901618>

Design Principles for Smallsat SARs

Conference Paper · August 2018

CITATIONS

7

READS

1,077

1 author:



[Anthony Freeman](#)

California Institute of Technology

271 PUBLICATIONS 6,456 CITATIONS

SEE PROFILE

Some of the authors of this publication are also working on these related projects:



Polarimetric SAR [View project](#)



Deep Space cubesat and Smallsat Missions [View project](#)

Tuesday SSC18-V-01

Design Principles for Smallsat SARs

Anthony Freeman

Jet Propulsion Laboratory, California Institute of Technology
4800 Oak Grove Drive, Pasadena, CA 91109; (818) 354 1887
anthony.freeman@jpl.nasa.gov

ABSTRACT

Synthetic Aperture Radar (SAR) is by now a mature remote sensing technique to obtain spatially-resolved radar measurements of terrain. Currently, SAR image data are readily available from an ever-expanding multitude of SAR satellites in Earth orbit. Many spaceborne SAR systems currently in use or planned for the near-term are multi-functional: their designs tend to maximize the menu of image modes available to the end user. They also follow fairly conventional design principles, laid down decades ago, that lead almost inevitably to large antennas and even larger spacecraft. This raises the question: how does one go about designing a SAR system that fits in a Smallsat (<200 kg) form factor?

The design principles for Smallsat SARs outlined in this paper have been developed over a twenty-year period in architecting Earth-orbiting SARs such as NASA/JPL's NISAR and ESA's Biomass mission, as well as planetary SAR mission concepts. Example mission concepts following this approach will be presented at the end of the paper. These include an S-Band Smallsat geodetic constellation to measure surface deformation, as called for by the 2018 National Academy Decadal Survey for Earth Observation from Space. Another example is a Ka-band cubesat-sized system designed to detect changes on Earth's surface.

INTRODUCTION

Many would consider this a golden age for Synthetic Aperture Radar. There are multiple civil-use SAR systems currently in Earth orbit, with several being the second or third generation of their kind. SAR images appear everywhere, used in a wide variety of applications from oceanography to forestry, agriculture and disaster response. Data are available from a wide range of systems developed by space agencies around the world. The European Space Agency's Sentinel-1a and -1b¹, launched in 2014 and 2016 continue a long series of C-Band SAR observations begun by ERS-1 in 1991, followed by ERS-2² in 1995 and then the ASAR on board Envisat³ in 2002. The Canadian Space Agency's Radarsat-2⁴, still operating more than 10 years after its launch in 2007, is expected to be superseded by the Radarsat constellation⁵ in 2018. Radarsat-2 itself continues a series of C-Band SAR observations begun by Radarsat-1⁶ in 1995. The German Space Agency's TerraSAR-X⁷ and Tandem-X⁸ satellites, launched in 2007 and 2010, have generated very precise digital topographic maps using X-Band SAR interferometry⁸. The Spanish government launched a clone of TerraSAR-X – the PAZ SAR mission¹⁰ – in February 2018. The Korean Kompsat-5, launched in 2013, carries an X-Band SAR¹¹. The Italian Space Agency's COSMO/SkyMed¹² constellation of four X-Band SAR satellites was launched from 2007 to

2010, and is still operational. The Indian Space Agency's RISAT-1 C-Band SAR¹³ was launched in 2012, joining their X-Band RISAT-2 SAR satellite¹⁴ launched in 2009. The Japanese Space Agency began observing the Earth using L-Band SAR in 1992 with JERS-1¹⁵, followed by PalSAR onboard ALOS-1 in 2006, then ALOS-2¹⁶ in 2014. The Argentinian Space Agency plans to launch two L-Band SAR satellites called SAOCOM-1 and -2¹⁷ in 2018 and 2019. The UK Space Agency, in partnership with Surrey Space Technology Limited, has developed an S-Band SAR called NovaSAR-S¹⁸, with plans to launch in 2018.

What do all these spaceborne SAR systems have in common? All (with the exception of RISAT-2) have planar array antennas, often with electronic beam steering to provide multiple look directions. All are multi-mode radars, with high, medium and low spatial resolution options, wide and narrow swaths, diverse combinations of polarizations, some exotic modes such as Spotlight for enhanced along-track resolution, and even split antenna modes for moving target discrimination. Second or third generation Earth-orbiting SAR satellites tend to have more modes added; Radarsat-2 for example advertises 20 imaging modes, whereas Radarsat-1 had just 6. The Envisat SAR had a total of 11 different imaging modes (including multiple polarization options), whereas ERS-1 had only 2. These

SAR systems also tend to follow design principles laid out in the frequently cited 1991 reference work by Curlander and McDonough¹⁹.

So what will the next generation of spaceborne SARs be like? Some SAR designers are pursuing a path towards ever more complex systems, with even more modes, using techniques such as MIMO-SAR²⁰ and TOPSAR²¹ that subdivide the antenna and generate multiple waveforms to stretch the bounds of what is possible for a SAR to do²². Actively steered phased array antennas, with complex beam steering networks and exquisitely designed timing sequences are integral to such designs.

In the US, the Earth Science community recently expressed its needs for SAR measurements over the next ten years in a decadal survey released by the National Research Council²³. That document, commonly referred to as ESAS 2017, identifies a need for more rapid revisit times to coherently monitor surface deformation on the Earth's surface, at intervals much less than current SAR satellites provide (less than one week, and as frequent as daily). Coherency from measurement to measurement is key: and can only be achieved using near-identical SAR systems flown in near-identical orbits. But to make such measurements by deploying constellations of large SAR platforms is prohibitively expensive: they may be more affordable if Smallsat SAR solutions can be found. So how does one go about designing a science-capable SAR system that fits in a Smallsat (<200 kg) form factor?

To reduce the size of a Synthetic Aperture Radar sensor and flight system, the first priority is to diminish the size of the antenna to the smallest possible dimensions. In an earlier paper²⁴, "The Myth of the Minimum SAR Antenna Area Constraint", the author and colleagues showed how smaller antennas than conventional approaches can be used in SAR design and still achieve reasonable performance. Resources other than volume are also often tightly constrained on Smallsat missions: available power, thermal control, and data rates for example. Rules of thumb can be used to govern the selection of the radar sensor parameters so that these resources are not over-taxed. Innovation is achieved through the application of such constraints in architecting the Smallsat SAR, which tends to result in lower costs.

This paper defines an alternative approach to the design of the next generation of SAR systems, one that stresses simplicity over complexity, starts from mission objectives before defining the system capabilities, and applies constraints that tend to reduce other factors that drive cost, such as mass, power usage, and data rates.

The design principles that flow from this approach are defined in this paper. Following this design philosophy, the application of the synthetic aperture technique is not central to the observation methodology, it is merely one element of the observing system design. It may not always even be necessary to form what most people would think of as an image when using the SAR technique. The next generation of Synthetic Aperture Radars may then be called simply radar sensors, in the same way that digital cameras with CMOS detectors are known simply as digital cameras.

As examples of where this design philosophy can lead, few are probably aware that the NASA/JPL Soil Moisture Active-Passive (SMAP) mission, launched in 2015, flew a circular scanning radar that sharpened up its spatial resolution using synthetic aperture processing²⁵. It is perhaps more widely known that the Cryosat-2 radar altimeter sensor launched in 2010 employs a SAR mode known as Delay-Doppler altimetry to improve its along-track spatial resolution²⁶. Similarly, NASA/JPL's SWOT radar altimeter sensor will provide improved altimeter spatial resolution by combining interferometry with the synthetic aperture technique²⁷. All three of these examples are focused on a quite specific set of science objectives.

This paper is organized to contrast the traditional approach to SAR design with the more unconventional approach preferred by the author. Example use cases that apply the Design Principles are described towards the end of the paper.

THE TRADITIONAL APPROACH TO SAR DESIGN

Most traditional SAR designs start through the definition of a side-looking, stripmap SAR mode that can achieve the highest desired spatial resolution (δx and δy), while providing the widest possible swath width (W_g), over a range of incidence angles (η) that provide significant (and meaningful) radar backscatter return (σ or σ^0). The geometry is illustrated in Figure 1. For stripmap SAR, the best-case along-track spatial resolution is given by the well-known expression:

$$\delta x \geq L_a/2 \quad (1)$$

where L_a is the physical length of the SAR antenna in the along-track dimension. Maximizing the swath covered at this resolution, while avoiding undesirable ambiguous echoes, gives rise to the well-known constraint on SAR antenna area:

$$A_a = W_a L_a > \frac{K4V\lambda R_m}{c} \tan \eta \quad (2)$$

where W_a is the antenna width in the across-track dimension, V is the speed of the platform, c is the speed of light, R_m is the range to the center of the swath, and K is a safety factor to build margin into the design, usually set in the range 1-3. For a spaceborne SAR, the orbital altitude defines the platform speed V , and once the incidence angle is selected that determines R_m . The wavelength is usually chosen for sensitivity to variations in surface phenomena that provide meaning, e.g. soil moisture in the case of L-Band ($\lambda \sim 24$ cm), or

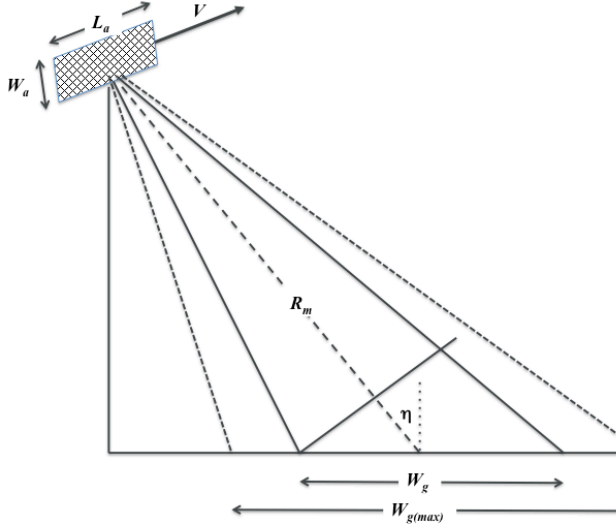


Figure 1: Simplified illustration of the geometry for a side-looking spaceborne SAR, with some key parameters indicated on the sketch.

ocean surface waves in the case of C-Band ($\lambda \sim 6$ cm) or shorter wavelengths. The SAR designer's degrees of freedom following equations (1) and (2) are therefore tightly constrained, and most spaceborne SAR antenna designs end up being fairly long (between 5 and 15 m) in the along-track dimension and short in the across-track dimension (between 0.8 and 2 m).

Another factor in setting the antenna dimensions is imposed by a requirement to have adequate Signal-to-Noise ratio (SNR). For a given σ^0 , it can easily be shown that the SNR has an upper bound¹⁹:

$$SNR_{max} \propto \frac{P_t L_a W_a^2 \tau_p}{B_n} \quad (3)$$

where P_t is the peak transmit power, τ_p is the duration of the transmitted pulse, and B_n is the noise bandwidth of the radar receiver. These three parameters can be highly constrained, so to achieve a reasonable SNR the SAR designer is often forced towards an antenna solution with relatively large L_a and W_a values.

Once the antenna has been sized for the stripmap mode, if the SAR has a phased array antenna other modes are then often incorporated that take advantage of adaptive beam steering: Spotlight mode for higher along-track spatial resolution at the expense of along-track swath extent; ScanSAR or TOPSAR modes for wider swath coverage at the expense of coarser along-track spatial resolution. In some SAR systems the antenna is subdivided to generate images of the same scene separated by milliseconds in time to characterize motion within the scene. Polarization diversity (e.g. HH or VV, HH and HV) may be incorporated if the antenna and receiver chain supports acquisition of radar returns in more than polarization configuration. [Polarization diversity makes the radar data easier to interpret for some applications and is therefore added to provide more information content about the scene.] Thus fairly conventional stripmap SAR designs with a planar, phased array antenna can be (and very often are) adapted to support many different modes of operation.

A NON-CONVENTIONAL APPROACH TO SAR DESIGN

A) Minimize the Antenna Length

In an earlier paper²⁴, it was shown that equation (2) is really a 'soft' constraint, one that only strictly applies when the SAR designer seeks at the same time to both minimize the along-track resolution δx and maximize the swath width W_g for which data are collected. In cases where coarser spatial resolutions and narrower swath widths are acceptable, shorter SAR antennas are not only possible but have been flown in space. In fact the fundamental constraint can be expressed as:

$$\frac{W_g}{\delta x} < \frac{c}{2V \sin \eta} \quad (4)$$

which does not include the antenna dimensions at all. [Hence the title of that reference: "The Myth of the SAR Minimum Antenna Area Constraint".]

A key insight from²⁴ is that one can design SARs that transmit pulses at Pulse Repetition Frequencies (PRFs) smaller than the Doppler bandwidth B_D , provided it is possible to relax the spatial resolution and/or swath width. The Doppler bandwidth is the spread of Doppler frequencies seen in the radar returns by a SAR in side-looking geometry, within the limits of the terrain illuminated by the SAR antenna. It is usually approximated by:

$$B_D \approx 2V/L_a \quad (5)$$

an expression that conventional SAR designs often use as a lower limit on the PRF. A shorter antenna length L_a

tends to increase the Doppler Bandwidth, which increases the required PRF value.

The implications of using a smaller PRF than suggested by (5) were reported in [Freeman, 2006]²⁸ and are illustrated in Figure 2, in which the strength of the ambiguous echoes in the along-track direction (the Signal-to-Azimuth Ambiguity ratio in dB) is plotted for a range of PRFs smaller than Doppler bandwidth B_D , against the fraction of the available bandwidth used in processing. This result is plotted for a uniformly fed planar array antenna, but is easily extended to other antenna configurations. To illustrate how the SAR designer might use this result, consider the case when the PRF is set at 85% of B_D . Figure 2 shows that reasonable azimuth ambiguity levels of < -23 dB can still be obtained if only 40% of the available bandwidth is used in SAR processing (azimuth compression). This means that the best achievable along-track resolution is now no longer the $L_a/2$ limit given in (1), but it is degraded by a factor $(0.85 \cdot 0.4) = 0.34$. For the case where $L_a = 5$ m, for example, the best achievable along-track resolution is now, therefore, ~ 7.4 m (instead of 2.5 m). This is roughly equivalent to the best-case spatial resolution from a SAR antenna 15 m long.

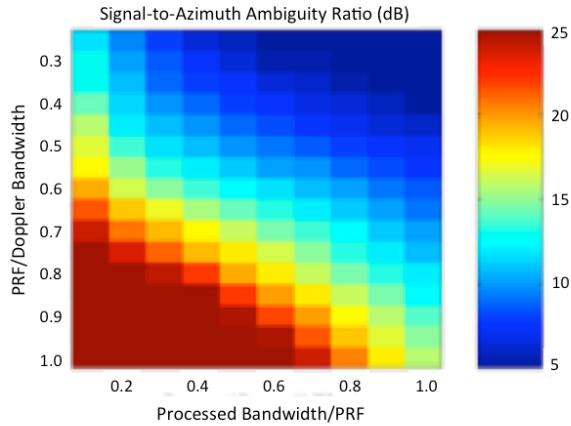


Figure 2: Signal-to-Azimuth Ambiguity ratios in dB as a function of the PRF expressed as a fraction of the Doppler Bandwidth and the Processed Bandwidth expressed as a fraction of the PRF. Signal and ambiguous echo levels were integrated over the available processing bandwidth to generate these results. A uniformly fed planar array with side-looking geometry was assumed.

So what are the trade-offs involved in shortening the antenna length? There is another (upper) limit on the PRF that says to avoid significant ambiguous echoes in range the pulse repetition interval ($1/\text{PRF}$) must be smaller than the time it takes to collect returns from the

recorded swath on the ground¹⁹. This can be expressed as:

$$\text{PRF} < \frac{c}{2W_g \sin \eta} \quad (6)$$

So using a smaller antenna often means reducing the amount of swath it is possible to record. As an example, take a SAR antenna of dimensions 15 m X 1.5 m, optimized for best-case stripmap-mode spatial resolution $\delta x = 7.5$ m, and a swath width W_g of ~ 100 km⁶. Shrinking the antenna length to 5 m would reduce the useful swath by about a factor of 3, and the SNR by a similar factor, after equation (3).

B) Minimize the Antenna Width

Narrowing the antenna width W_a significantly extends the *illuminated* swath $W_{g(\max)}$ on the ground, but there is a severe penalty to be paid in SNR, which has a W_a^2 dependence, again from equation (3). If the SAR designer tries to extend the *recorded* swath W_g , then equation (6) comes into play, as a consequence constricting the *PRF*. But as seen in Figure 2 and the associated discussion, the *PRF* cannot be reduced arbitrarily without impacting the level of along-track ambiguities, and/or the along-track spatial resolution.

C) Over-illuminate the Swath

As discussed above, narrowing the antenna width W_a significantly extends the *illuminated* swath $W_{g(\max)}$ but there is in general no need to make the *recorded* swath $W_g = W_{g(\max)}$. It can be set significantly smaller to reduce the instantaneous data rate (which is proportional to swath width), a significant concern for planetary SAR systems in particular²⁹⁻³⁴. It may also be necessary to restrict the recorded swath W_g to those regions within $W_{g(\max)}$ where the range ambiguities are at acceptable levels [this depends on the precise shape of the antenna pattern in elevation] A SAR system design with $W_g \ll W_{g(\max)}$ is inefficient, since one is illuminating terrain with radar pulses but not collecting the radar echoes. However, it is not specifically prohibited by any other design consideration.

D) Select the Lowest Mass Density Antenna

It is well-known that spacecraft mass tends to be a strong driver of system cost³⁵. Figure 3 shows that for SAR systems spacecraft mass (and therefore system cost) correlates well with antenna mass when the SAR is the dominant payload. So to reduce overall system cost the priority is to reduce the antenna mass.

What drives antenna mass? One factor is captured in Figure 4, which shows that SAR systems with more

acquisition modes trend towards having greater antenna mass (with a couple of exceptions). SAR systems with low mass antennas tend to have just one or two acquisition modes (Seasat, JERS-1, ERS-1, MicroXSAR³⁶, and Biomass³⁷). The two exceptional cases shown: NovaSAR-S and RISAT-2, have a very compact phased array antenna, and a phased array feed/deployable mesh reflector antenna, respectively. All of the other systems, with antenna mass values of around 400 kg and higher, are phased array antennas. What's going on here is partly that SAR designers like to add more modes to keep up with the state-of-the-art (no-one wants their system to be less capable than 'the competition'). Active phased array antennas allow more SAR modes to be implemented, so phased array antennas have become the norm. If at the same time the system is required to have the widest possible swath, and best possible along-track resolution that leads to massive, bulky antennas.

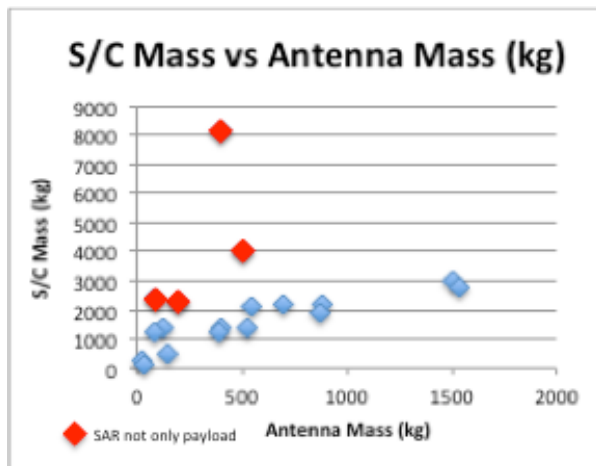


Figure 3: Total spacecraft mass vs SAR antenna mass for 17 civil spaceborne (Earth-orbiting) SAR systems. Systems where the SAR is or was not the only significant remote sensing payload are indicated as red diamonds.

The SAR systems that group towards the bottom left-hand corner of Figure 4 use different antenna technologies in place of active phased arrays: passive microstrip patches (Seasat and JERS-1), slotted waveguides (ERS-1 and MicroXSAR), and passive deployable reflectors (Biomass). Reflectarray antennas, now demonstrated in space on JPL's ISARA³⁸ and MarCO³⁹ cubesats, also offer potential as lighter SAR antennas, but at the expense of restricted mode flexibility.

Reinforcing this argument, as illustrated in Figure 5, the SAR antennas with the lowest mass density (kg/unit area) tend to be those that do not use active phased array technology.

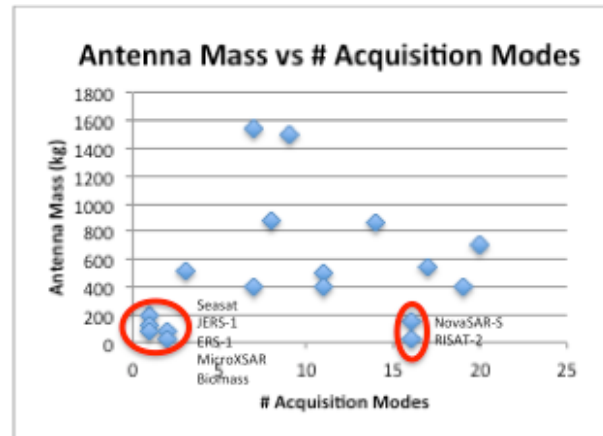


Figure 4: SAR antenna mass plotted against the number of different acquisition modes for 17 civil spaceborne (Earth-orbiting) SAR systems.

Note that RISAT-2, a close cousin of the Israeli TecSAR system⁴⁰, has a phased array feed with a passive deployable reflector, which allows multiple acquisition modes while still achieving low mass. This approach may be unique in that it allows low mass density antennas to have quite sophisticated data acquisition modes, such as SweepSAR⁴¹, which was baselined in JPL's design for the DESDynI SAR mission⁴²⁻⁴⁴, and has since evolved into the current NISAR project⁴⁵.

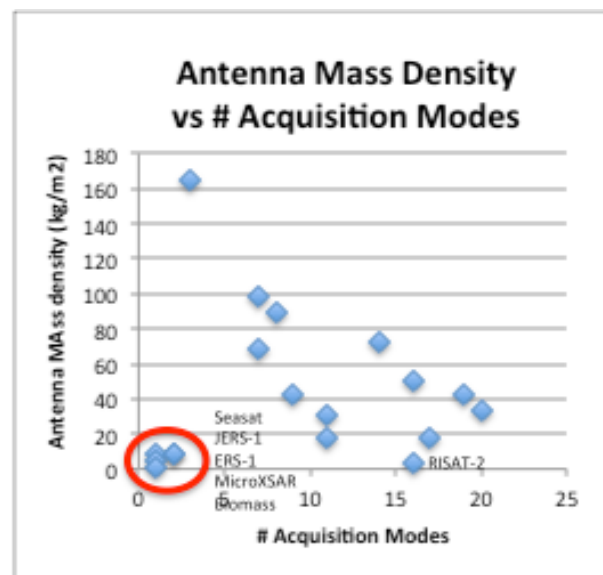


Figure 5: SAR antenna mass density plotted against the number of different acquisition modes for 17 civil spaceborne (Earth-orbiting) SAR systems.

E) *Choose the smallest possible number of Imaging Modes*

The discussion above leads to this design principle.

F) *Add polarization diversity only when needed to meet the majority of system requirements*

The addition of polarization diversity with the ability to acquire multiple polarizations simultaneously, adds science value to the measurements, and can often be the only way that the primary science objectives of the mission can be met. Biomass, DESDynI and NISAR are notable examples of this.

Adding polarimetry complicates the system design however^{46,47} and often forces the SAR designer towards a phased array antenna solution, since that approach leads to a fairly straightforward implementation.

Compact or hybrid-pol architectures⁴⁸ can reduce the complexity when compared with fully polarimetric systems, and are compatible with reduced-mode system designs. Scientists who use SAR data have been slow to embrace this approach, though its implementation on recent missions such as RISAT-1¹³ and the upcoming Radarsat constellation⁵ may help turn that tide.

G) *Select a Data Rate that maximizes on-time per orbit*

The data rate for a SAR system can be represented as:

$$D_R = n \cdot \left(\frac{W_s}{c} + \tau_p \right) \cdot n_b f_s \cdot (PRF / PreSum) \cdot F_{OBP} \quad (7)$$

where n is the number of different channels (e.g. polarizations, multiple antennas for interferometry) for which the system collects data; W_s is the recorded swath width in slant range, n_b is the number of bits per sample; f_s is the sampling frequency - typically set to be at least 2X greater than the pulse bandwidth B_p ; the *PreSum* factor represents the amount of Doppler bandwidth that is actually captured (compared with the PRF)⁴⁹; and F_{OBP} represents the degree to which On-Board Processing (OBP), e.g. to form a SAR image, reduces the effective data rate.

If the SAR on-time per orbit is T_{on} seconds, and the maximum data volume that can be downlinked per orbit is D_{max} , then the metric that the SAR designer should seek to maximize is:

$$T_{on} = \frac{D_{max}}{D_R} \quad (8)$$

For a fixed downlink capacity, the degree of freedom here is in D_R , yielding several options:

- i. Reduce the number of channels n to the minimum possible (consistent with Design Principle *F* above)
- ii. Record data over a smaller swath width (consistent with Design Principle *C*)
- iii. Use a shorter pulse (this is not common)
- iv. Reduce the number of bits per sample, e.g. by using techniques such as BFPQ¹⁹
- v. Presum or prefilter to knock down the usable Doppler bandwidth, and therefore degrade the along-track resolution (see Design Principle *A*)
- vi. Perform On-Board Processing, forming a SAR image then multi-looking to reduce the effective data rate (may lose phase information in the process).

Option vi is attractive in many respects, since it can reduce the data rate significantly, but has not been widely adopted. This may be because the SAR designer pays the penalty that phase information is lost, eliminating one of the strongest and most unique applications of SAR data: repeat-pass interferometry or RPI. For RPI to work from repeat orbit to repeat orbit, one needs phase coherence, which is eliminated when a detected SAR image is formed, then multi-looked. RPI capability is often a baseline (i.e. non-negotiable) requirement for science-driven SAR measurements, such as those specified for Surface Deformation in NASA's ESAS 2017²³.

H) *Select an average power consumption that maximizes on-time per orbit (but beware thermal overload)*

The average DC power needed to operate a SAR system can be represented by:

$$P_{DC} = \left(\frac{P_t \tau_p PRF}{\epsilon} + P_{rec} \right) \cdot \frac{T_{on}}{T_{orbit}} \quad (9)$$

where P_t is the RF peak transmit power, ϵ represents the DC-RF conversion efficiency of the High-Power amplifier used to transmit (typically in the range 30-70%), P_{rec} is the DC power drawn by the receiver electronics, and T_{orbit} is the orbit period.

For a fixed amount of DC power available to operate the radar, eq. (9) suggests the SAR designer has the following degrees of freedom:

- i. Reduce the peak RF power – which will have the effect of increasing the minimum noise-equivalent sigma-naught¹⁹
- ii. Select the most efficient transmitter option available
- iii. Select receiver electronics that use less power (consistent with Design Principle *F*)

The note of caution to the SAR designer here is that all the DC transmit power that is not converted to RF generates heat instead. That heat has to be dissipated if the radar electronics are not to exceed operating temperature. This often limits the SAR on-time.

PUTTING THE DESIGN PRINCIPLES INTO PRACTICE

The author has been involved with quite a few SAR system concept designs over the years, some that have been proposed to NASA, and at least one to ESA³⁷. In each case, wherever possible the design principles outlined above have been followed. Proposed concepts are often very well-defined, but complete design descriptions do not always appear in the literature. Table 1 captures the features of seven examples of SAR designs that the author has been personally involved in, with references indicating where further details have been published. Note that, except for DESdynI, in all these examples the minimum number of modes was preferred. Active, phased array antennas, have been avoided, which allowed lower mass solutions.

Table 1: SAR Concept Designs^{42, 43 and 50-58}

SAR Design Concept	Features	Antenna Type [Mass Density]
Mars UHF SAR (2003) ⁵⁰⁻⁵²	Polarimetry, BFPQ, PreSum, Over-illumination of Swath, single mode	Passive, deployable reflector [2.0 kg/m ²]
Biomass precursor (2004) ⁵³	Short antenna, Polarimetry, BFPQ, PreSum, single mode	Passive, deployable reflector [1.9 kg/m ²]
DESDynI (2009) ^{42,43}	Polarimetry, multiple modes, SweepSAR	Passive, deployable reflector with a phased array feed [3.6 kg/m ²]
VERITAS (2014) ^{54,55}	Single polarization, Short antennas, OBP, single mode	Slotted Waveguide [10.5 kg/m ²]
Ka-band Cubesat SAR (2016) ⁵⁶	Short antenna, single mode of operation	Slotted Waveguide or Microstrip Patch or <i>Reflectarray</i> [7.9 kg/m ²]
S-band Smallsat SAR constellation (2017) ⁵⁷	Single polarization, Short antenna, BFPQ, PreSum, single mode	Slotted Waveguide or Microstrip Patch [10.0 kg/m ²]
VHF radar sounder (2017) ⁵⁸	PreSum, OBP, single mode	Yagi [9.9 kg with 10 m crossed dipoles]

The Ka-Band cubesat SAR concept in Table 1, which targets observations of ocean surface wave features was described briefly in a conference presentation at the 2016 Cubesat Developer's Workshop in San Luis

Obispo, CA. It addresses a unique challenge to design a SAR that can fit within a 12U cubesat volume. The approach adopted by the author was to use a very short antenna (Design Principle *A*) with the widest possible extent (30 cm) at Ka-Band (Principle *B*). A reflectarray antenna was the lowest mass density option available (Principle *D*). This SAR has a single imaging mode (Principle *E*) and just one polarization (Principle *F*). A BFPQ of (8:4) and a Presum factor of 3 to were selected to knock down the data rate (Principle *G*), but thermal constraints limited the on-time per-orbit for this concept to just 3 mins (Principle *H*).

The spacecraft concept for this Ka-Band cubesat SAR is illustrated in Figure 6 and the SAR design parameters are summarized in Table 2.

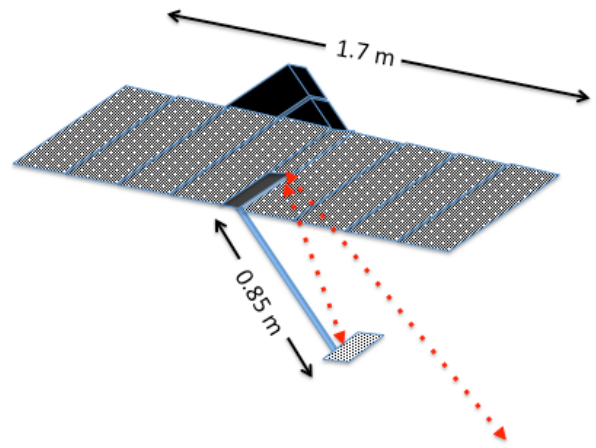


Figure 6: Ka-Band SAR concept shown in deployed configuration. Design stows into a 12U volume.

Table 2: Ka-Band 12U Cubesat SAR⁵⁶

Parameter	Value
Orbit altitude	400 km
Center Frequency	35 GHz
Incidence angle	30 degrees
Transmit peak RF power	240W
DC Power	160W
Pulse length	50 microsec
Antenna Dimensions	1.7 X 0.3 m
F/D ratio	0.7
Bandwidth	30 MHz
Data rate	104 Mbps
On-time per orbit	3 mins
Downlink rate	40 Mbps
Noise-equivalent sigma-zero	-17 dB
Spatial resolution/# of looks	10 m/2
Swath width	15 km

SUMMARY AND CONCLUSIONS

The Design Principles set out in this paper lay out an alternative path to the conventional approaches that appear in the standard literature on SAR systems. They also offer an alternative to the ever-expanding plethora of modes that most SAR designers seem to strive towards. They have been developed and applied over the last two decades by the author and others at JPL to novel SAR concept designs. They are particularly well-suited to the design and realization of lower-mass solutions, especially Smallsat SAR concepts⁵⁶⁻⁵⁸.

Acknowledgments

The author has had the privilege of working with some of JPL's finest radar system designers in the two decades spent developing this set of design principles. The list includes my colleagues Scott Hensley, Louise Veilleux, Ernesto Rodriguez, Curtis Chen, Bryan Huneycutt, Stephen Horst and the late Bill Johnson and Rolando Jordan, who are both sadly missed. It has also been my pleasure to work with some outstanding antenna designers over the years, including Richard Hodges, Mark Thomson and more recently, Nacer Chahat.

The research described in this paper was carried out at the Jet Propulsion Laboratory, California Institute of Technology, under a contract with the National Aeronautics and Space Administration.

References

1. Snoeij, P., et al, "C-SAR Instrument Design for the Sentinel-1 Mission", IEEE Radar Conference, May 2010
2. Attema, E., Desnos, Y-L., Duchossois, G., "Synthetic Aperture Radar in Europe: ERS, Envisat and Beyond", Johns Hopkins APL Technical Digest, Volume 21, Number 1, 2000.
3. Desnos, Y-L., et al, "ASAR – Envisat's Advanced Synthetic Aperture Radar", ESA Bulletin 102, May 2000.
4. Fox, P. Luscombe, A. P., Ali, Z., "The Radarsat-2 Mission, New Modes and Techniques," Proceedings of IAC (International Astronautical Congress), Houston, Tx, Oct 2002.
5. Séguin, G., "A Canadian Constellation of C-Band SAR Satellites," Proceedings of the 56th IAC 2005, Fukuoda, Japan, Oct 2005.
6. Ahmed, S. Parashar, S., Langham, E., McNally, J., "RADARSAT Mission Requirements and Concept," Canadian Journal of Remote Sensing, Vol. 19, No. 4, Nov-Dec 1993.
7. Werninghaus, R., Balzer, W., Buckreuss, S., Mittermayer, J., Mühlbauer, P., Pitz, W., "The TerraSAR-X Mission," Proceedings of EUSAR 2004, Ulm, Germany, May 2004
8. Krieger, G., Moreira, A., Hajnsek, I., Werner, M., Fiedler, H., Settelmeier, E., "The TanDEM-X Mission Proposal," Proceedings of the ISPRS Hannover Workshop 2005, Hannover, Germany, May 2005.
9. Krieger, G., Zink, M., Moreira, A., "TanDEM-X: A Radar Interferometer with two Formation Flying Satellites," Invited paper, Proceedings of the 63rd IAC (International Astronautical Congress), Naples, Italy, Oct 2012.
10. "The Paz satellite: a defense and security solution provided by Astrium Espana," URL: <http://www.astrium.eads.net/en/news2/the-paz-satellite-a-defence-and-security-solution-provided-by-astrium-espana.html>, Feb 2009.
11. Lee, S-R., "Overview of KOMPSAT-5 Program, Mission, and System," Proceedings of IGARSS (IEEE International Geoscience and Remote Sensing Symposium) 2010, Honolulu, HI, USA, July 2010.
12. Di Lazzaro, M., Angino, G., Piemontese, M., Capuzi, A., Leonardi, R., "COSMO-SkyMed: The Dual-Use Component of a Geospatial System for Environment and Security," Proceedings of the 2008 IEEE Aerospace Conference, Big Sky, MT, USA, March 2008.
13. Misra, T., S. S. Rana, V. H. Bora, N. M. Desai, C. V. N. Rao, Rajeevjyothi, "SAR Payload of Radar Imaging Satellite (RISAT) of ISRO," Proceedings of EUSAR 2006, Dresden, Germany, May 2006.
14. <https://earth.esa.int/web/eoportal/satellite-missions/r/risat-2>
15. Nomoko, Y., et al, "Japanese Earth Resources Satellite-1 Synthetic Aperture Radar", Proceedings of the IEEE, VOL. 79, NO. 6, June 1991.
16. Shimada, M., "Advanced Land Observation Satellite (ALOS) and its follow-on satellite, ALOS-2," Proceedings of the 4th International POLinSAR 2009 Workshop, ESA/ESRIN, Frascati, Italy, Jan 2009.

17. Frulla, L., et al, "SAOCOM Mission Overview", 2011 CEOS SAR Calibration and Validation Workshop Fairbanks, AK, Nov 2011.
18. Cohen, M., et al, "NovaSAR-S Low Cost Spaceborne SAR Payload Design, development and deployment of a new benchmark in spaceborne radar", IEEE Radar Conference, Seattle, WA, May 2017.
19. Curlander, J. C. and [McDonough, R. N., *Synthetic Aperture Radar Systems and Signal Processing*, publ. John Wiley, 1991.](#)
20. Krieger, G., "MIMO-SAR: Opportunities and Pitfalls", IEEE Transactions on Geoscience And Remote Sensing, VOL. 52, NO. 5, May 2014.
21. Zan, F. and [Monti Guarnieri, A., "TOPSAR: Terrain Observation by Progressive Scans", *IEEE Transactions on Geoscience and Remote Sensing*, Vol. 44, *Issue: 9*, Sept 2006.](#)
22. Younis, M., Krieger, G., and Moreira, A., "MIMO SAR Techniques and Trades", European Radar Conference (EuRAD), Oct 2013.
23. 2017-2027 *Decadal Survey for Earth Science and Applications from Space* (ESAS 2017), The National Academies Press, Feb 2018.
24. Freeman, A., W. T. K. Johnson, B. Honeycutt, R. Jordan, S. Hensley, P. Siqueira, and J. Curlander, "The Myth of the Minimum SAR antenna area constraint," IEEE Trans. Geosci. Remote Sensing, vol. 38, pp. 320–324, Jan 2000.
25. Spencer, M., Chan, S., Veilleux, L., and Wheeler, K., "The Soil Moisture Active/Passive (SMAP) Mission Radar: a Novel Conically Scanning SAR," Proceedings of the 2009 IEEE Radar Conference, Pasadena, CA, USA, May 2009.
26. Raney, R. K., "The Delay/Doppler Radar Altimeter," IEEE Transactions on Geoscience and Remote Sensing, Vol. 36, No 5, Sept. 1998.
27. Rodriguez, E., and Esteban-Fernandez, D., "The Surface Water and Ocean Topography Mission (SWOT): The Ka-band Radar Interferometer (KaRIn) for water level measurements at all scales," Proceedings of the SPIE Remote Sensing Conference, Toulouse, France, Vol. 7826, Sept 2010.
28. Freeman, A., On Ambiguities in SAR Design, Proc. EUSAR 2006, Dresden, Germany, June 2006.
29. Freeman, A. and Smrekar, S., VERITAS – a Discovery-class Venus surface geology and geophysics mission, 11th Low Cost Planetary Missions Conference, Berlin, Germany, June 2015.
30. Hensley, S., S. Smrekar, S. Shaffer, M. Paller, H. Figueroa, A. Freeman, R. Hodges, P. Walkemeyer, VISAR: A Next Generation Interferometric Radar for Venus Exploration, Venus Lab and Technology Workshop, Houston, TX, Jan. 2015.
31. Freeman, A. and Campbell, B.A., A UHF SAR Mission to Mars, presented at ASAR 2003 Workshop. Ottawa, Canada: Canadian Space Agency, June 2003.
32. Campbell, B.A., A. Freeman, L. Veilleux, B. Honeycutt, M. Jones, R. Shotwell, A P-band radar mission to Mars, Proc. IEEE Aerospace Conference, 2004.
33. Campbell, B.A., T. Maxwell, and A. Freeman, Mars orbital SAR: Obtaining geologic information from radar polarimetry, J. Geophys. Res., 109, doi:10.1029/2004JE002264, 2004.
34. Campbell B. A., Grant J. A. Plaut J. J., Freeman A., Return and Human Exploration Benefits of an Orbital Imaging Radar for Mars, Concepts and Approaches for Mars Exploration, Lunar and Planetary Institute, Houston, TX, June 2012.
35. Wertz, J. R., et al, Methods for Achieving Dramatic Reductions in Space Mission Cost, Reinventing Space Conference, Los Angeles, CA March 2011.
36. Saito, H., et al, Engineering-Model Results of Compact X-Band Synthetic Aperture Radar, 4S Symposium, May 2018.
37. European Space Agency, "Biomass: Report for mission selection," ESA Communication Production Office, Noordwijk, The Netherlands, SP-1324/1, Available: <https://earth.esa.int/web/guest/documentlibrary/browse-document-library/-/article/biomass-report-for-missionselection-an-earth-explorer-to-observe-forest-biomass> (2012)
38. Hodges, R., Shah, B., Muthulingham, D., and Freeman, A., ISARA – Integrated Solar Array and Reflectarray Mission Overview, Annual

- AIAA/USU Conference on Small Satellites, August 2013.
39. Klesh, A. and Krajewski, J., MarCO: Cubesats to Mars in 2016, 29th Annual AIAA/USU Conference on Small Satellites, SSC15-III-3 (2015)
 40. Naftaly, U. and Levy-Nathansohn, R., Overview of the TECSAR Satellite Hardware and Mosaic Mode, IEEE GRSL, Vol. 5, No. 3, July 2008
 41. Freeman, A., G. Krieger, P. Rosen, Younis, M., W. T. K. Johnson, Huber, S., R. Jordan, and Moreira, A., SweepSAR: Beam-forming on Receive using a Reflector-Phased Array Feed Combination for Spaceborne SAR, Proc. Radarcon '09, Pasadena, CA, May 2009.
 42. Freeman, A., et al, Deformation, Ecosystem Structure, and Dynamics of Ice (DESDynI), Proc. EUSAR 2008, Friedrichshafen, Germany, June 2008.
 43. Freeman, A. et al, DESDynI – A NASA Mission for Ecosystems, Solid Earth, and Cryosphere Science, Proc. PolinSAR 2009, Frascati, Italy, January 2009.
 44. Johnson, W. T. K., Rosen, P., Hensley, S., and Freeman, A., Radar Design for the DesdynI Mission, Proc. Radarcon '09, Pasadena, CA, May 2009.
 45. <https://nisar.jpl.nasa.gov/>
 46. Freeman, A., On the Design of Spaceborne Polarimetric SARs, Proc. Radarcon '09, Pasadena, CA, May 2009.
 47. Raney, R. K., Freeman, A., and Jordan, R. L., Improved Ambiguity Performance with Quad-Pol SAR, IEEE TGRS, VOL. 50, NO. 2, Feb 2012.
 48. Raney, R. K. and Freeman, A., Hybrid-Polarity SAR Architecture, Proc. PolinSAR 2009, Frascati, Italy, January 2009.
 49. Freeman, A., A Digital Prefilter for MTI with SAR, Digital Signal Processing-84, Sept 1984.
 50. Freeman, A. and Campbell, B.A., A UHF SAR Mission to Mars, presented at ASAR 2003 Workshop. Ottawa, Canada: Canadian Space Agency, June 2003.
 51. Campbell, B.A., A. Freeman, L. Veilleux, B. Huneycutt, M. Jones, R. Shotwell, A P-band radar mission to Mars, Proc. IEEE Aerospace Conference, 2004.
 52. Campbell, B.A., T. Maxwell, and A. Freeman, Mars orbital SAR: Obtaining geologic information from radar polarimetry, J. Geophys. Res., 109, doi:10.1029/2004JE002264, 2004.
 53. Freeman, A., “Calibration of Linearly Polarized Polarimetric SAR Data Subject to Faraday Rotation,” *IEEE Transactions on Geoscience and Remote Sensing*, vol. 42, no. 8, pp. 1617–1624, 2004.
 54. Hensley, S., S. Smrekar, S. Shaffer, M. Paller, H. Figueroa, A. Freeman, R. Hodges, P. Walkemeyer, VISAR: A Next Generation Interferometric Radar for Venus Exploration, Venus Lab and Technology Workshop, Houston, TX, Jan. 2015.
 55. Freeman, A. and Smrekar, S., VERITAS – a Discovery-class Venus surface geology and geophysics mission, 11th Low Cost Planetary Missions Conference, Berlin, Germany, June 2015.
 56. Freeman, A., Hyon, J., and Waliser, D., The Cube-Train Constellation for Earth observation, 13th Annual Cubesat Developer’s Workshop, San Luis Obispo, April 2016.
 57. A Freeman, N Chahat, S-Band smallsat InSAR constellation for surface deformation science, Radar Conference (RadarConf), May 2017 IEEE, 0867-0872
 58. Freeman, A., Pi, X., Heggy, E., Radar Sounding Through the Earth’s Ionosphere at 45 MHz, IEEE Transactions on Geoscience and Remote Sensing 55 (10), 5833-5842, 2017